Chemosphere 184 (2017) 1270–1285

Contents lists available at ScienceDirect

Chemosphere

journal homepage: www.elsevier.com/locate/chemosphere

Resource efficiency analysis for photocatalytic degradation and mineralization of estriol using TiO_2 nanoparticles

Irwing M. Ramírez-Sánchez [a], Shea Tuberty [b], Mike Hambourger [c], Erick R. Bandala [d, *]

[a] Universidad de las Américas Puebla, Sta. Catarina Mártir, Cholula, Puebla, 72810, Mexico
[b] Department of Biology, Appalachian State University, Boone, NC, 28608, USA
[c] Department of Chemistry, Appalachian State University, Boone, NC, 28608, USA
[d] Division of Hydrologic Sciences, Desert Research Institute, 755 E, Flamingo Road, Las Vegas, NV, USA

HIGHLIGHTS

- The relationship between catalyst loading and temperature with •OH generation was assessed.
- The effect of temperature on •OH generation was fitted using the Arrhenius model.
- Initial E3 degradation rate was related to •OH generation in the system.
- E3 mineralization was feasible under different catalyst loading scenarios.
- Photocatalytic efficiency indices for heterogeneous photocatalytic process were proposed.

ARTICLE INFO

Article history:
Received 27 March 2017
Received in revised form
6 June 2017
Accepted 12 June 2017
Available online 14 June 2017

Handling Editor: W. Mitch

Keywords:
Hydroxyl radical
Resource efficiency
Arrhenius model
Estriol
Degradation
Mineralization

ABSTRACT

A resource efficiency analysis was developed that evaluated photocatalyst loading and temperature inputs, and assessed hydroxyl radical (•OH) production. Catalyst loading (Aeroxide® TiO_2 P25) between 1 and 1500 mg L^{-1} and temperatures between 5 and 50 °C were analyzed as input resources for •OH production. After, the best experimental conditions were used to degrade and mineralize estriol (E3). The analysis showed that a low catalyst concentration lead to poor absorption of radiation and a slow reaction. When high catalyst concentrations were tested, most of the radiation was absorbed, which produced results near the top of the slowing rate of •OH generation. Temperature was found a relevant resource for increasing interfacial transfer to facilitate •OH production following the Arrhenius model. Two indices to measure resource efficiency were proposed: 1) the •OH generation index (OHI) and 2) the initial degradation efficiency (IDE). OHI was used to measure the efficiency of a catalyst using photonic flux to generate •OH production. IDE evaluated the relationship between the photocatalytic reactor set-up, catalyst, and E3 degradation. It was observed that 1.18 •OH was produced when a photon interacts with a photocatalyst particle when a load of 5 mg L^{-1} of photocatalyst is used at 20 °C. It was found that at initial time, 2.4 •OH was generated in the systems to produce a degradation of one E3 molecule when using a photocatalyst load of 20 mg L^{-1} at 20 °C. Additionally, it was demonstrated that E3 mineralization was feasible under different catalyst loading scenarios.

1. Introduction

Pharmaceutical and personal care products (PPCPs) are chemicals that have been present in water and wastewater for many decades. However, they have only recently been recognized as potentially significant water pollutants (Czech and Rubinowska, 2013) and have been classified as emerging contaminants by the toxicological community. Natural attenuation or conventional municipal wastewater treatment processes either only partially remove or are incapable of removing PPCPs from water (Desbrow et al., 1998). The PPCPs determined to be endocrine-disrupting compounds (EDCs)—which include the natural and synthetic estrogens: estrone (E1), 17β-estradiol (E2), estriol (E3), 17α-ethynylestradiol (EE2), mestranol, and quinestrol—are of significant concern for humans and ecosystems. The presence of natural

* Corresponding author.
E-mail address: erick.bandala@dri.edu (E.R. Bandala).

http://dx.doi.org/10.1016/j.chemosphere.2017.06.046
0045-6535/

estrogens in drinking water and wastewater effluents has been well-documented (Chen et al., 2007; Kuch and Ballschmiter, 2001). Common sources of these estrogens include human excretion, livestock waste, pharmaceuticals, and effluent from municipal wastewater treatment plants (Williams and Brooks, 2012). The concentration of natural estrogens in raw wastewater has been reported to be as high as 670 ng L^{-1} for estrone, 161 ng L^{-1} for estradiol, and 845 ng L^{-1} for estriol (Liu et al., 2015). In humans, exposure to estrogen for hormonal therapy has been correlated with an increased risk of breast, uterine, and testicular cancer (Cavalieri et al., 2000) and a factor for developing diabetes mellitus (Nadal et al., 2009). In wildlife, studies have shown that estrogens were responsible for disrupting phenotypic expression in alligator eggs (Hileman, 1994), the immune and reproductive systems of grey seals (Dimogerontas and Liapi, 2014), vitellogenin expression in male fish (Desbrow et al., 1998; Hileman, 1994), and the endocrine systems of invertebrates (Matozzo et al., 2008; Oetken et al., 2004; Souza et al., 2013).

Because estrogens were identified in wastewater effluents (Desbrow et al., 1998), biological, physicochemical, and advanced treatment processes have been studied to determine suitable methods to remove the activity of these compounds from water (Silva et al., 2012). Advanced oxidation processes using titanium dioxide as photocatalyst have been demonstrated to be effective for the degradation of estrogens in water. Coleman et al. (2000) reported one of the first works on photocatalytic degradation of natural estrogens using TiO_2. Since then, several studies have investigated the degradation of estrogens using UV-activated TiO_2 in simple to complex matrices, such as ultrapure water (Coleman et al., 2004, 2005a, 2005b; Han et al., 2012; Karpova et al., 2007; Li and Sun, 2014; Malygina et al., 2005; Mao et al., 2013; Mboula et al., 2015; Nakashima et al., 2002, 2003; Tanizaki et al., 2002), surface water (Benotti et al., 2009), and wastewater effluents (Dimitroula et al., 2012; Fanourgiakis et al., 2014; Frontistis et al., 2012; Nasuhoglu et al., 2012; Zhang et al., 2012).

The photocatalytic activity of TiO_2 is based upon the absorption of a photon with energy greater or equal to the band gap energy, inducing the formation of an electron-hole pair that allows reaction with surface adsorbed chemical species such as a water molecule, molecular oxygen, or organic molecules (Nakata et al., 2012). In instances where water is found in much greater abundance than organic reductants, it can be expected that valence band holes will oxidize water to produce hydroxyl radicals (•OH). Concurrently, conduction band electrons can reduce O_2 to superoxide, leading to the formation of additional hydroxyl radical (Fujishima et al., 2007). The scheme in Fig. 1 shows the events that may occur at a TiO_2-water interface upon photoactivation (Nosaka and Nosaka, 2013).

Estrogen photocatalytic degradation has been suggested to proceed by both a direct pathway by reacting with the positively charge holes on the catalyst surface and an indirect pathway induced by •OH (Li and Sun, 2014). The starting point of the photocatalytic oxidation of estrogens has been suggested at the phenol moiety (Ohko et al., 2002) occurring via abstraction of the benzylic hydrogen by the •OH radical or the attack of the •OH group to form quinone-type compounds (Coleman et al., 2004, 2005a, 2005b). For this reason, measuring •OH generation is valuable to determine the activity of TiO_2 for estrogen degradation.

The most studied estrogens, sorted in order of decreasing literature, are estradiol (E2) > estrone (E1) > ethynylestradiol (EE2) > estriol (E3) because of their estrogenic potencies and the concentrations detected in fresh and wastewater (Ramirez-Sanchez et al., 2017). E3 is of interest for this study because it was predicted that 1) E3 would be more frequently detected in fresh and wastewater because of the increased use of estriol in hormone replacement therapy and 2) the E3 concentration would be 2.39 times greater than the average concentration of estrone and estradiol (Liu et al., 2015) but the monitored values of E3 would be lower than the expected concentrations based on human excretion rates (Kostich et al., 2013).

Estriol degradation was demonstrated using undoped TiO_2 under different conditions: TiO_2 Aeroxide® P25 immobilized on a glass borosilicate spiral reactor (Coleman et al., 2005a, 2005b), TiO_2 immobilized on glass beads (Mizuguchi et al., 2006), TiO_2 Aeroxide® P25 (Li Puma et al., 2010), and TiO_2 grown in a glass matrix (Kushwaha et al., 2015). However, there are few documented experimental trials devoted to measuring the efficiency of •OH radicals for E3 degradation and mineralization (Ramirez-Sanchez et al., 2017).

When photocatalytic processes are studied, there are important input resources such as photocatalyst loading, temperature and photon flux that should be considered when monitoring outcomes such as reactive oxygen species (ROS) production (e.g., •OH). The •OH generated from photoactivated TiO_2 can be directly measured by various technologies, such as pulse laser spectroscopy (Fischer et al., 1985), electron paramagnetic resonance (EPR) (Brezová et al., 2003), or chemiluminescent methods (Maki et al., 2009). However, using scavenging reagents or probes (Brezonik and Arnold, 2011) is an easy alternative to assess •OH production. Among probes available, *N*,*N*-dimethyl-4-nitrosoaniline (pNDA, also named RNO) bleaching is one based on UV–visible

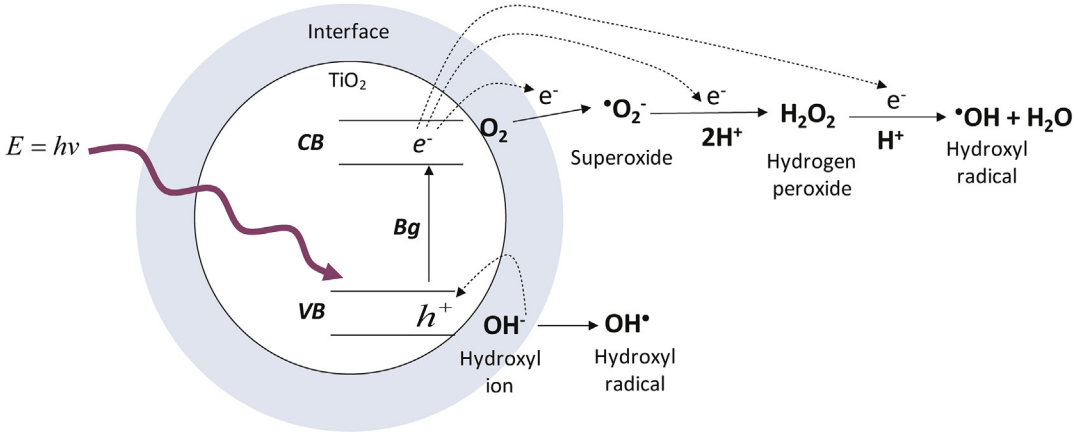

Fig. 1. Scheme of the •OH generation on photoactivated TiO_2.

spectroscopy analysis. pNDA bleaching has been used to detect •OH in biochemical systems (Bors et al., 1979; Pastore et al., 2000), electrochemical treatment (Barashkov et al., 2010; Feng et al., 2003; Guitaya et al., 2014; Muff et al., 2011; Quiroz et al., 2014), UV/H_2O_2 process (Kwon et al., 2009), Fenton reactions (Komagoe et al., 2008; Sun et al., 2015), TiO_2 aqueous suspensions (Kim et al., 2013; Zang et al., 1997), and TiO_2 supported systems (Simonsen et al., 2010).

The goal of this work was to assess and set up the optimal experimental conditions for E3 degradation and mineralization by first monitoring •OH generation using pNDA as scavenging reagent, while investigating catalyst loading (1–1500 mg L^{-1} of Aeroxide® TiO_2 P25), and temperature (5–50 °C).

2. Materials and methods

2.1. Reagents

Estriol (E3, $C_{18}H_{24}O_3$, ≥97%), *N*,*N*-dimethyl-4-nitrosoaniline (pNDA, $C_8H_{10}N_{20}$, 97%), 1,10-phenanthroline ($C_{12}H_8N_2$, ≥99%), sodium acetate anhydrous (CH_3COONa, >99%), iron(III) sulfate hydrate ($Fe_2(SO_4)_3 \cdot 7H_2O$ 97%), potassium oxalate monohydrate ($(COOK)_2 \cdot H_2O$, 99%), ethylenediaminetetraacetic acid ($(HO_2CCH_2)_2NCH_2CH_2N(CH_2CO_2H)_2$, >99.4), iron(II) sulfate heptahydrate ($FeSO_4 \cdot 7H_2O$, >99.0%), potassium dichromate ($K_2Cr_2O_7$, >99.0%), diphenylamine ($(C_6H_5)_2NH$, > 99%), salicylic acid (2-(HO) $C_6H_4CO_2H$, >99.0%), and glycine (NH_2CH_2COOH, >98.5%) were obtained from Sigma-Aldrich. The structural formulas and aqueous absorption spectra of E3 and pNDA are shown in Fig. 2a and b, respectively. Sulfuric acid, HPLC grade methanol, and water were purchased from Fremont Industries. All the chemicals were used as received without further purification.

Aeroxide® TiO_2 P25 (previously known as Degussa® P25, 50 ± 15 $m^2 g^{-1}$ specific surface area, 21 nm average primary particle size, 80:20 anatase/rutile weight ratio, more than 99.5% of TiO_2, according to the manufacturer) was obtained from Evonik Industries and used as the photocatalyst without intentional superficial modifications or doping.

2.2. Photoreactor setup

A photoreactor was used in all the experiments of photon flux, pNDA bleaching-•OH generation (based on catalyst loading and temperature dependence), and E3 degradation and mineralization. Two 15 W black light lamps (GE, F15T8 BLB, product code: 35885) were centered horizontally over the photoreactor. The emission spectra of the lamps were obtained using a spectrophotometer with a webcam with CMOS, without a UV optical filter, and a diffraction grating of 1000 lines/mm, as described by Lorenz (2014) and Widiatmoko et al. (2011). Irradiation intensity was determined using a UVX Digital Radiometer (UVP).

The photoreactor was a 318 mL cylindrical water-cooled jacketed glass vessel with an inner height of 102 mm and an inner diameter of 63 mm, as shown in Fig. 3. The horizontal position of the photoreactor was constant for all experiments. A lab jack lifting platform was used to adjust the vertical position of the photoreactor for experiments using varying photon flux, but the vertical position was constant for the pNDA bleaching-•OH generation, E3 degradation, and mineralization experiments. The vertical position was measured from the bottom of the lamp to the water-free surface of the photoreactor. The temperature of the reaction mixture was controlled using a thermostatic bath (Polystat, Cole-Parmer). Experiments involving the effects of temperature were conducted between 5 and 50 °C, and other experiments were kept at 20 °C. The overall system was placed in a closed box to avoid the effects of any other natural or artificial radiation sources.

2.3. Photonic flux determination

The ferrioxalate chemical actinometer was used to quantify the photon flux of incident radiation into the photoreactor. It was selected because of its sensitivity (Parker, 1953) and its ability to work at a wavelength range between 250 and 500 nm (Kuhn et al., 2004), which covers the spectrum emissions of the GE F15T8 BLB used in this work. The ferrioxalate actinometer was based on measuring the photoreduction of ferric to ferrous ions using spectrophotometric determination of the 1,10-phenanthroline complex ($[Fe(phen)_3]^{2+}$) at 510 nm (Montalti et al., 2006). The experimental extinction coefficient for the ferrous complex was $Abs_{\lambda=510\ nm} = 10304.3$ $[Fe(phen)_3]^{2+}$. The procedure for preparing the actinometric solution was described elsewhere in the literature (Murov et al., 1993).

Briefly, 100 mL of the potassium ferrioxalate actinometric solution was prepared by mixing iron (III) sulfate and potassium oxalate solutions. The temperature was 20 ± 0.5 °C, and then the potassium ferrioxalate solution was irradiated for three minutes. An aliquot of the irradiated solution was withdrawn and mixed with a buffered solution of 1,10-phenantholine to develop the complex agent. All actinometric solutions were prepared in an amber volumetric flask.

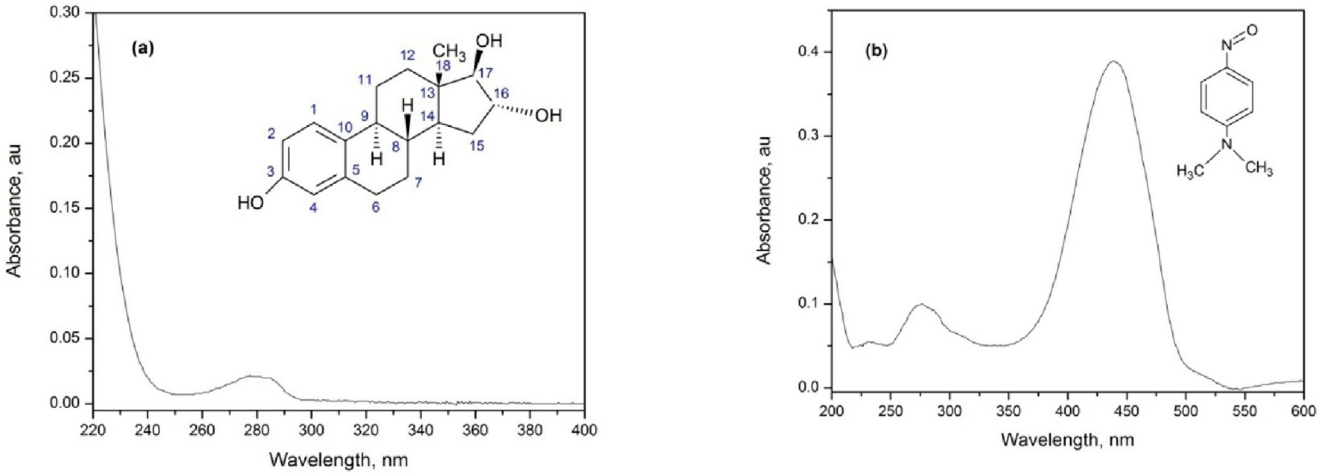

Fig. 2. Structural formula and absorbance spectrum of a) E3 (10 μM, and pH 6), and b) pNDA (10 μM, and pH 6).

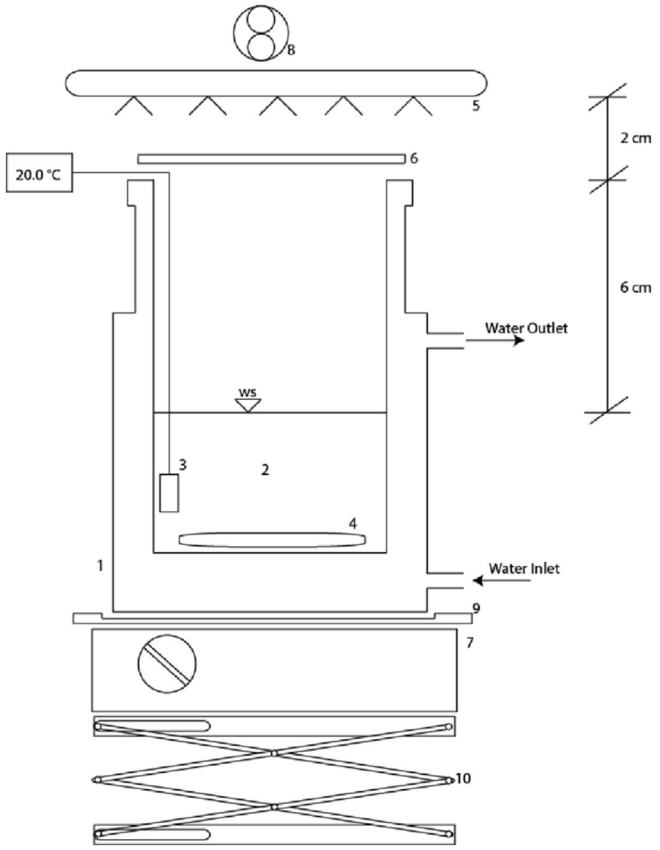

Fig. 3. Water-cooled, jacketed glass photoreactor: 1) glass reactor, 2) testing solution, 3) temperature probe, 4) spin bar, 5) black light lamp, 6) optical filter (if needed), 7) stirring plate, 8) cooling fan, 9) horizontal position template, and 10) lab jack lifting platform.

2.4. Hydroxyl radical generation

To obtain the efficiency of the photocatalytic system and support the notion of •OH participation in E3 degradation and mineralization in the aqueous phase, pNDA was used as an •OH scavenger (or probe) based on results from previous works (Barashkov et al., 2010; Bors et al., 1979; Kim et al., 2013; Martínez-Huitle et al., 2004; Zang et al., 1997). The 10 μM pNDA test solution was prepared and initially adjusted to pH 6.0 ± 0.1 using NaOH or HCl as needed because pNDA coloration is sensitive to pH changes (Muff et al., 2011). No buffer solution was used because it could compete with the pNDA scavenger for generated •OH radicals. The end value of pH for the reactions was verified using the discharged pNDA bleaching mixture. pNDA bleaching was measured using a UV–visible spectrophotometer (Hatch DR/4000U) at 440 nm (see Fig. 2b). Experiments using catalyst loading between 1 and 1500 mg L^{-1} at 20 °C were carried out to evaluate the effect of TiO_2 load on •OH generation. Experiments using different temperature values between 5 and 50 °C were carried out using the same photocatalyst concentration of 20 mg L^{-1}. For all experiments, after adding the catalyst, the solution was mixed for 20 min in the dark (without radiation) and an aliquot was withdrawn and centrifuged to evaluate pNDA absorption onto the TiO_2 particles. The cap was then removed to allow the two GE F15T8 BLB lamps to illuminate the system. Aliquots from the irradiated pNDA solution were withdrawn after certain periods and centrifuged at 6000 rpm for 15 min (Biofuge Primo, Sorvall) to remove the photocatalyst before they were measured in a UV–visible spectrophotometer. The aliquots without the photocatalyst were directly measured in the UV–visible spectrophotometer.

2.5. Photolysis and photocatalytic degradation of E3

The initial estriol concentration was selected to be 10 μM because of the sensitivity of the analytical techniques used in this work and because this research was part of a project that focused on removing E3 in water using sequentially coupled membrane filtration and TiO_2 photocatalytic process. The concentration of 10 μM was chosen in order to stay below the limit of E3 solubility in water, which previously was reported as between 11.1 μM (Hurwitz and Liu, 1977) and 45.1 μM (Silva et al., 2012; Ying et al., 2002). All experiments with E3 solution were temperature controlled to 20 °C and the solution did not appear cloudy.

Estrogen working solutions were stored in amber flasks. The E3 solution was prepared by stirring at room temperature in the absence of radiation for six hours to dissolve approximately 2.88 mg of E3 in 1 L of distilled water, or $[E3] = \frac{2.88\times10^{-3}\text{g}}{288.38\ \text{gmol}^{-1}1\text{L}} = 10\mu\text{M}$. For every experiment, 100 mL of this E3 solution were added to the reactor and the temperature was set to 20 °C. Depending on the initial water conditions, the initial pH value for all of the experiments was adjusted to 6.0 ± 0.1 using NaOH or HCl as needed. The initial pH was adjusted to generate a similar surface charge of the photocatalyst (e.g., TiO_2) in all of the experimental runs (Fernández-Ibáñez et al., 2000). For all experiments using E3, a dark period (without radiation) of 20 min was allowed during which E3 and the photocatalyst were stirred without radiation source to ensure adsorption equilibrium in the solution. Similar experimental conditions were carried out as described for •OH generation experiments. Additionally, the aliquots taken from E3 solution were filtered using a 0.1 μm syringe filter (Millex-VV, Millipore) to avoid damaging the HPLC column.

2.6. Analytical methods

Estriol was monitored using a High Performance Liquid Chromatograph (HPLC) system (Waters 1515) equipped with a UV detector (Waters 2787) that had an injection volume of 20 μL. The quantification of E3 was performed using the isocratic analytical mode and an Inertsil® ODS-3 column (150 mm × 4.6 mm, 5 μm, 25 °C). The UV detector was set at λ = 280 nm based on the E3 maximum absorbance shown in Fig. 2a. The mobile phase was methanol (49%) and distilled water (51%) at a flow rate of 1 mL min^{-1}. The resulting retention time was 10 min and the limit of E3 detection was 0.1 μM (0.029 mg L^{-1}). The total organic carbon (TOC) concentration of the water samples was determined using a Shimadzu TOC-L CPN and the limit of E3 detection was also 0.1 μM (0.029 mg L^{-1}). The band gap energy of TiO_2 was obtained from diffuse reflectance spectra using Video Barelino with integrating sphere coupling to spectrophotometer Varian Conc with baseline of $BaSO_4$.

3. Results and discussion

3.1. Photoreactor radiative characterization

Lamp emissions were characterized for emission spectra, photon flux, and intensity. The emission spectra detector was calibrated using a fluorescent lamp, obtaining a correlation R^2 = 0.9997 (see Fig. 4a). For this lamp, a broad emission band (Fig. 4b) was found between 356 and 410 nm with a peak emission at 387 nm.

The band gap of Aeroxide TiO_2 P25 was found to be 3.3 eV

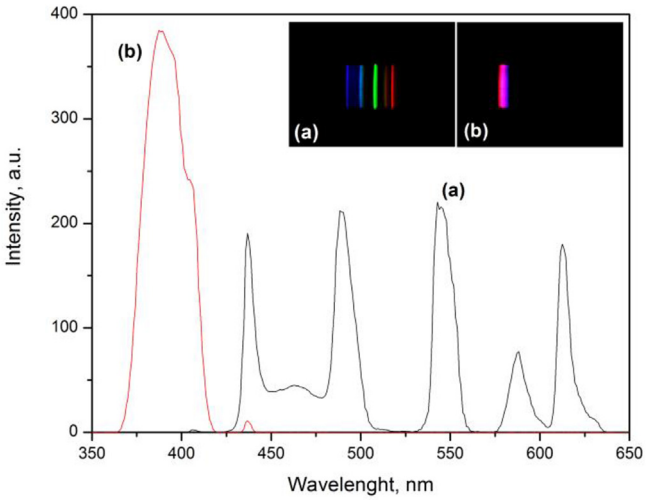

Fig. 4. Emission spectrum and intensity graph for a) the fluorescent lamp and b) the F15T8 BLB black light lamp.

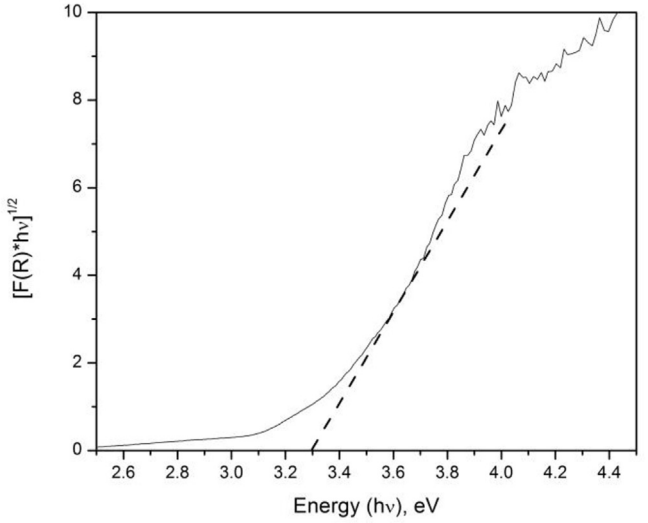

Fig. 5. Determination of the band gap energy for Aeroxide TiO_2 P25.

(376 nm) as shown in Fig. 5. The F15T8 BLB black light lamps were selected due to the strong spectral overlap between the emission band noted above and the absorption spectrum of Aeroxide TiO_2.

Actinometric characterization was found to have a linear dependence with the vertical position of the photoreactor. This can be described by $I = -1.4d + 39.6$—where I is light intensity (μEinstein min^{-1}) estimated for the volume and geometry of the photoreactor (Murov et al., 1993) and d is the distance from the lamps to the water-free surface in the photoreactor (cm)—and $R^2 = 0.994$, as shown in Fig. 6. Changing the photoreactor's vertical position by one centimeter produced a variation of 1.4 μEinstein min^{-1}. The radiation intensity chosen for all experiments was 28.1 μEinstein min^{-1}.

The position of photoreactor (Fig. 3) allowed samples to be withdrawn safely because there was a distance of 6 cm from the water-free surface to the edge of the photoreactor and 2 cm from the edge of the photoreactor to lamp surface, which was 8 cm from the lamp. At the selected position, radiative intensity was measured at 1500 μW cm^{-2} using a radiometer.

3.2. The effect of TiO_2 concentration on hydroxyl radical generation

To avoid misinterpreting between pNDA photolysis and photocatalytic pNDA bleaching, a photolysis experiment was developed under lamp radiation without a catalyst. The results for the photolysis experiments with pNDA were the only ones showing a zero-order kinetics with a straight line of $[pNDA][pNDA_0]^{-1} = -0.0008t\text{-}1.003$ (Fig. 7). Such zeroeth order kinetics are reasonable for a photochemical process operating at low photon flux since light availability will limit the rate of reaction. This assumption follows Simonsen et al. (2010) who found that pNDA bleaching using only UV light followed zero order kinetics. The present data are not sufficient to unambiguously rule out a first order kinetic for the direct photolysis. However, this zeroeth order assumption gave the better fit to the data. After 300 min of photolysis, 20% of the initial concentration of pNDA had been degraded and the initial reaction rate of pNDA photolysis bleaching was found to be 8×10^{-3} μM min^{-1}.

pNDA bleaching has been demonstrated to be useful for measuring the photocatalytic performance of TiO_2 (Kim et al., 2013; Simonsen et al., 2010; Zang et al., 1997). This method has some advantages:

1) it is selective of the reaction of pNDA with •OH (Kraljic and Trumbore, 1965);
2) it has a high reaction rate between pNDA and •OH on the order of 10^{10} M^{-1} s^{-1} (Farhataziz, 1977; Zang et al., 1997);
3) it is easy to observe bleaching at 440 nm following Beer's Law (Fig. 8 shows pNDA bleaching form yellowish to transparent solution); and
4) there is a 1:1 stoichiometry according to Equation (1) (Simonsen et al., 2010) which means that one •OH can bleach one pNDA molecule.

The photochemical bleaching of pNDA in the presence of UV-illuminated TiO_2 can be seen in Fig. 8. Equation (1) depicts a feasible reaction accounting for pNDA bleaching and equation (2) provides a kinetic expression for this reaction.

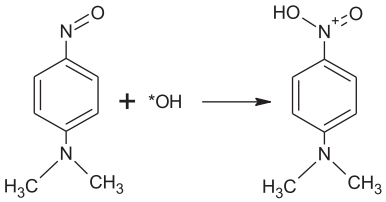

(1)

The pNDA photocatalytic bleaching could be modeled by a first order equation (Muff et al., 2011) expressed by Equation (2) and for derivation is obtained Equation (3):

$$-\frac{dpNDA}{dt} = k[^{\cdot}OH]_{ss}[pNDA] = k_1[pNDA] \quad (2)$$

$$[pNDA] = [pNDA_0]e^{-k_1 t} \quad (3)$$

where [pNDA] is the concentration of pNDA, k_1 pseudo-first-order constant, and $[\text{•OH}]_{ss}$ is the steady-state concentration of hydroxyl radical (•OH). Initial velocity (r_0) rate was obtained by evaluation of k_1 in Equation (3) followed by evaluation of Equation (4) at initial time (t = 0). Half-life was obtained through evaluation of Equation (3) when $[pNDA] = [pNDA_0]/2$ obtaining Equation (5).

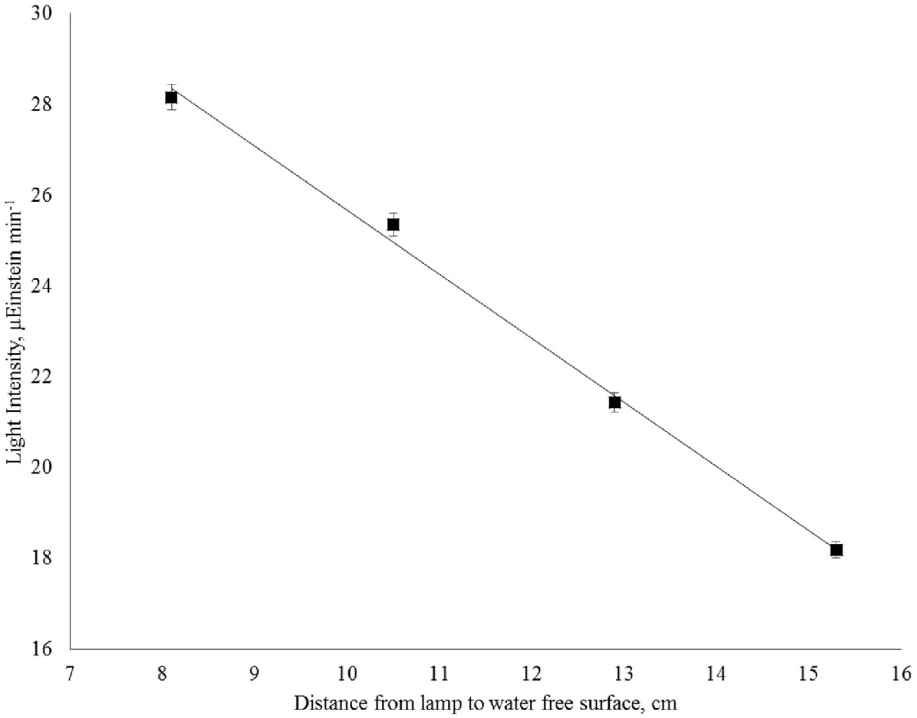

Fig. 6. Photon flux in the photoreactor as a function of distance to the radiation source.

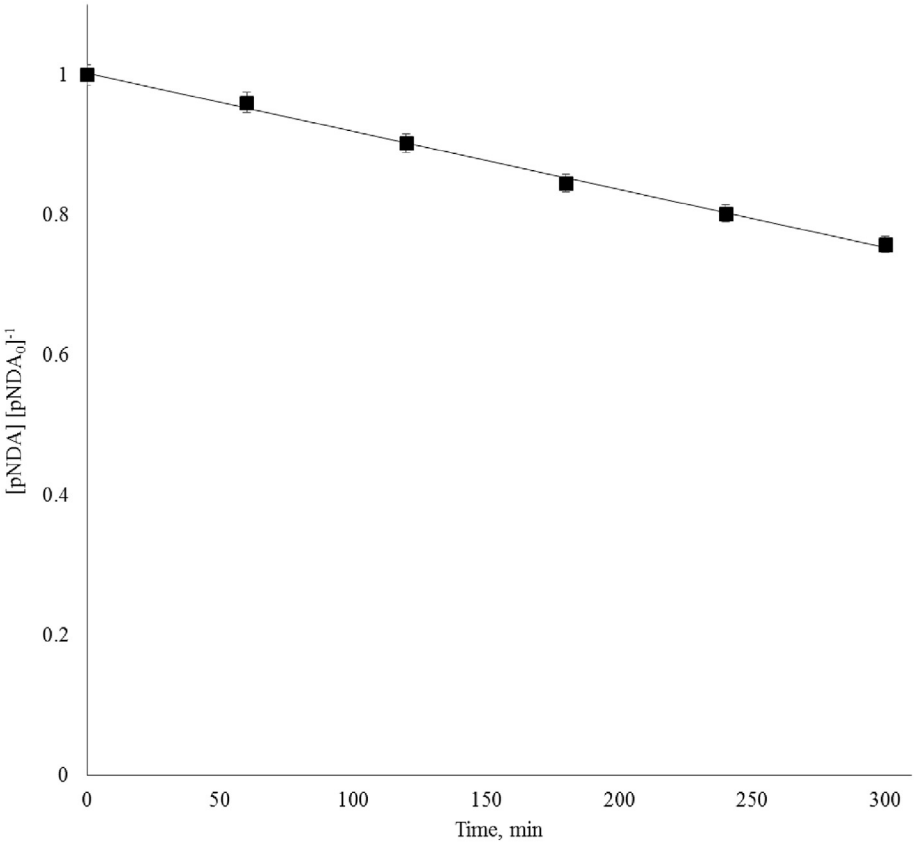

Fig. 7. Photolysis of pNDA bleaching (10 µM, pH 6, 20 ± 0.5 °C, Lamp GE F15T8 BLB).

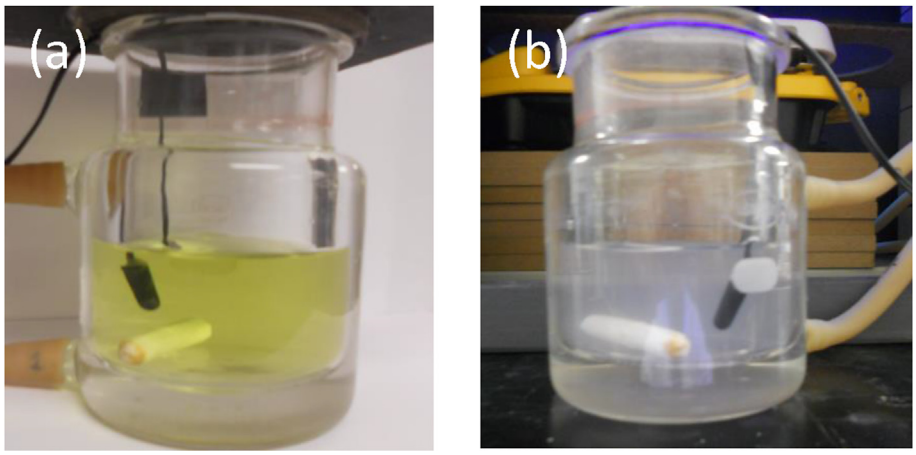

Fig. 8. pNDA with catalyst a) before and b) after UV exposure.

$$\left.\frac{d[pNDA]}{dt}\right|_{t=0} = r_0 = k_1[pNDA] \quad (4)$$

$$t_{1/2} = \frac{\ln(2)}{k_1} \quad (5)$$

Photocatalytic bleaching of pNDA under different TiO_2 loading concentrations from 1 to 1500 mg L^{-1} followed a pseudo-first-order reaction (k_1) according to Equation (3), which is shown in Fig. 9.

All the tested catalyst loads showed pNDA bleaching to be faster than the bleaching rate in the photolysis experiment (Fig. 7).

It was observed that the pseudo-first-order rate constant, k_1, in Table 1 shows an increase from 1 to 320 mg L^{-1} and a decrease after 320 mg L^{-1} of catalyst loading (Fig. 10). Increases in the reaction rate constant by an increase in the photocatalyst load between 1 and 360 mg L^{-1} may be related to the increase in the number of surface active sites within the TiO_2 particles, which was previously suggested by Giraldo et al. (2010). Further increases in the photocatalyst load beyond 360 mg L^{-1} did not show any further increase in the reaction rate, possibly because some the catalyst particles

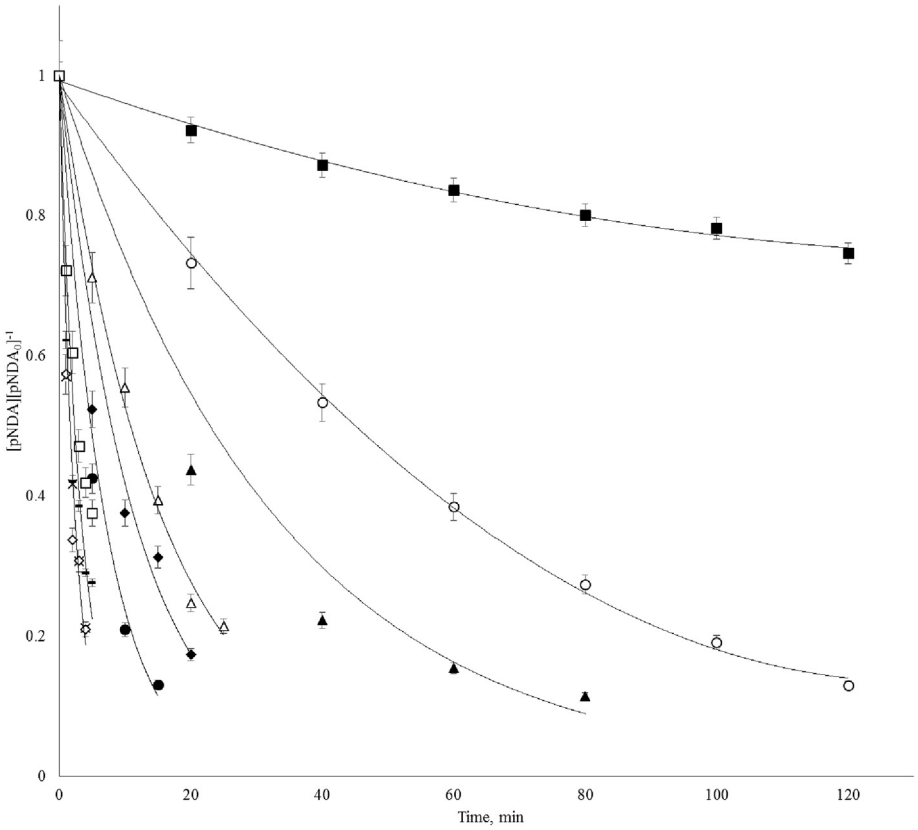

Fig. 9. Photocatalytic pNDA bleaching (10 μM, pH 6, 20 ± 0.5 °C, Lamp GE F15T8 BLB) using ■ 1 mg L^{-1}, ○ 5 mg L^{-1}, ▲ 10 mg L^{-1}, Δ 20 mg L^{-1}, ◆ 40 mg L^{-1}, ● 160 mg L^{-1}, □ 320 mg L^{-1}, 640 mg L^{-1}, ▬ 1000 mg L^{-1}, and ✖ 1500 mg L^{-1} with pseudo-first-order model (——) according Equation (3).

Table 1
Kinetics of hydroxyl radical generation by photocatalytic pNDA bleaching.

TiO_2 load, mg L^{-1}	$pNDA_0$, μM	k_1 min^{-1}	Inverse fluence (cm^2 mJ^{-1})[a]	R^2	Initial velocity rate, r $\mu M^{\bullet}_{OH}$ min^{-1}	Half-life, min	OHI, $^{\bullet}OH$ $photon^{-1}$ g^{-1}
1	10	0.003	(3.33×10^{-5})	0.949	0.03	266.6	0.93
5	10	0.02	(2.22×10^{-4})	0.998	0.17	41.8	1.18
10	10.5	0.03	(3.33×10^{-4})	0.935	0.32	23.0	1.13
20	7.7	0.06	(6.66×10^{-4})	0.988	0.49	10.8	0.88
40	7.9	0.09	(1.00×10^{-3})	0.954	0.69	7.9	0.61
80	9.4	0.14	(1.55×10^{-3})	0.971	1.35	4.8	0.60
160	9.1	0.40	(4.44×10^{-3})	0.976	3.66	1.7	0.82
320	9.7	0.42	(4.66×10^{-3})	0.933	4.05	1.7	0.45
640	8.2	0.30	(3.33×10^{-3})	0.875	2.45	2.3	0.14
1000	9.7	0.28	(3.11×10^{-3})	0.892	2.74	2.5	0.10
1500	8.2	0.22	(2.44×10^{-3})	0.944	1.78	3.2	0.04

Notes: Lamp type: F15T8BLB GE W; $\lambda_{max} = 365$ nm; photon flux = 28.1 μEinstein min^{-1}; radiative intensity = 1500 μW cm^{-2}; temperature = 20.0 ± 0.04 °C; and pH = 6.
[a] Inverse fluence was estimated using the incident fluence (not average fluence) rate computed from actinometry results.

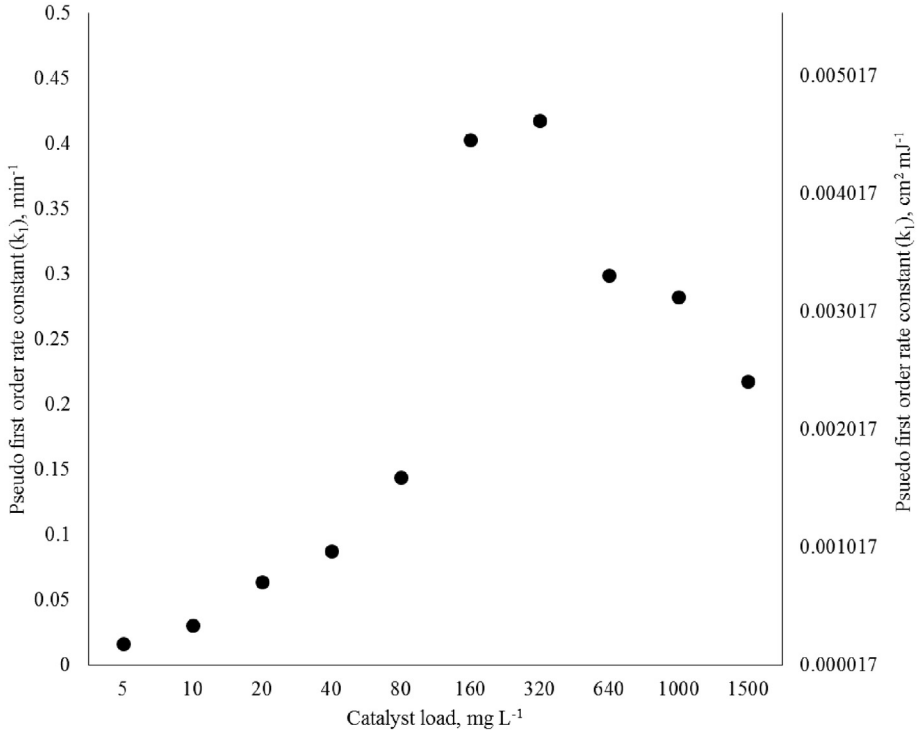

Fig. 10. Pseudo-first-order rate constant for pNDA photocatalytic bleaching (10 μM, pH 6, 20 ± 0.5 °C) by TiO_2 Aeroxide® P25 (1–1500 mg L^{-1}) under black light lamp (GE F15T8 BLB).

were fully illuminated and others were self-shading on the media, which reduced radiation penetration (Hapeshi et al., 2010) and increased radiation scattering (Han et al., 2012).

The maximum pseudo-first-order rate constant (k_1) was 0.42 min^{-1} (4.66×10^{-3} cm^2 mJ^{-1}) for 320 mg L^{-1} of photocatalyst loading. It was demonstrated that higher concentrations (over 320 mg L^{-1}) of the photocatalyst overload the system (Table 1), which leads to a decrease in the observed •OH generation and a reduction of resource efficiency related with radiation scattering, reduced radiation penetration, and agglomeration of the TiO_2 particles.

The quantum yield (ϕ) is defined as the number of times a molecule undergoes a given event per absorbed photon, which is shown in Equation (6). In TiO_2 heterogeneous photocatalytic experiments, quantum yield is often difficult to estimate because it is problematic to differentiate absorbed light from scattered light. The extent of light scattering by the catalyst particles depends on a number of physicochemical properties e.g. particle size, pH, surface charge, ion strength, and catalyst loading. Consequently, it is a non-trivial task to fairly assess the number of absorbed photons as required for a quantum yield determination.

$$\Phi = \frac{number\ of\ reacted\ molecules}{number\ of\ photons\ absorbed} \tag{6}$$

To overcome this issue, we propose an alternative to express the observed productivity of the photocatalytic process named •OH generation index (OHI). OHI considers photon flux and catalyst loading as inputs and observed •OH radicals as the output of the photocatalyst, described in Equation (7).

$$OHI = \frac{r_0}{I\delta} \tag{7}$$

where r_0 is the initial velocity rate (mol L^{-1} min^{-1}) obtained with Equation (4), I is the photonic flow (Einstein min^{-1}), and δ is the

photocatalyst load (g L^{-1}). Equation (8) shows the dimensional analysis to obtain OHI and the units are •OH photon^{-1} g^{-1}:

$$
\begin{aligned}
OHI[=]\frac{r_0}{I\delta}[=]\frac{mol_{OH}}{L{*}\min}\frac{\min}{Einstein}\frac{L}{g_{catalyst}}\frac{Einstein}{mol_{Photons}}\\
OHI[=]\frac{mol_{OH}}{mol_{Photons}{*}g}\\
OHI[=]\frac{6.022x10^{23}{\cdot}OH}{6.022x10^{23}Photons{*}g_{catalyst}}\\
OHI[=]\frac{{\cdot}OH}{Photons{*}g_{catalyst}}
\end{aligned}
\tag{8}
$$

The OHI intrinsically measures the fraction of photon flux being scattered or reflected by the particulate matter in the photocatalyst suspension. Therefore, the OHI was proposed as an observed measurement of resource efficiency in the process. It was found to be affected by the operational condition and experimental setup. The OHI was then plotted versus catalyst loading, as shown in Fig. 11. The highest OHI value found (Table 1) was 1.18 •OH photon^{-1} g^{-1}, which was achieved using 5 mg L^{-1} of photocatalyst loading.

At photocatalyst load values less than 5 mg L^{-1}, it is probable that some photons were not absorbed by the photocatalyst particles. For photocatalyst loads above 5 mg L^{-1}, almost all photons were absorbed but some photocatalyst particles shaded other particles within the photoreactor. The effect of TiO_2 shading could be demonstrated by the reduction in detected transmittance, as shown by the pNDA and TiO_2 effects in Fig. 12.

Considering the maximum OHI value, which was achieved using 5 mg L^{-1}, and the maximum •OH initial velocity rate (see Table 1), which was obtained using 320 mg L^{-1}, it could be proposed that the best resource efficiency for the experimental photocatalytic system is between these catalyst load values. The maximum OHI value measures the resource efficiencies for which the highest amount of •OH radicals were produce with the least amount of resources and the maximum pseudo-first-order constant value describes the conditions under which maximum •OH radical production can be achieved for the tested system.

The slow decrease in radical production efficiency observed for photocatalyst loads between 600 and 1500 mg L^{-1} is likely attributable to the interaction of radiation with the photocatalyst at the top of the solution, which generated a significant shading effect to the inner solution.

Maximum OHI was determined for photocatalytic, superficial, and morphological properties of Aeroxide® TiO_2 P25. It was found that different TiO_2 materials show variations in their photonic efficiency measurements because of differences in their crystalline array, particle size, and shape; differences in the density of hydroxyl groups on the particle surface and the number of water molecules hydrating the surface; and differences in the number and nature of trap sites (Serpone, 1997). Additionally, photonic efficiency could be affected by specific surface area and surface charge. Using OHI as an observed efficiency resource measurement, the optimal operational values could be selected to determine conditions under which the photocatalyst is fully activated by photons or to determine the amount of catalyst needed to produce the desired photocatalyst rate that allows for tradeoff resources between energy, catalyst load, and initial degradation rate.

3.3. The effect of temperature on hydroxyl radical generation of TiO_2

Although photocatalysis has been studied for many years, temperature dependence is unclear, which sometimes leads to misinterpretations of the experimental results. Liu et al. (2014) theorized that temperature affects the rate constant of interfacial electron transfer (k_{IT}) during a photocatalytic reaction following an

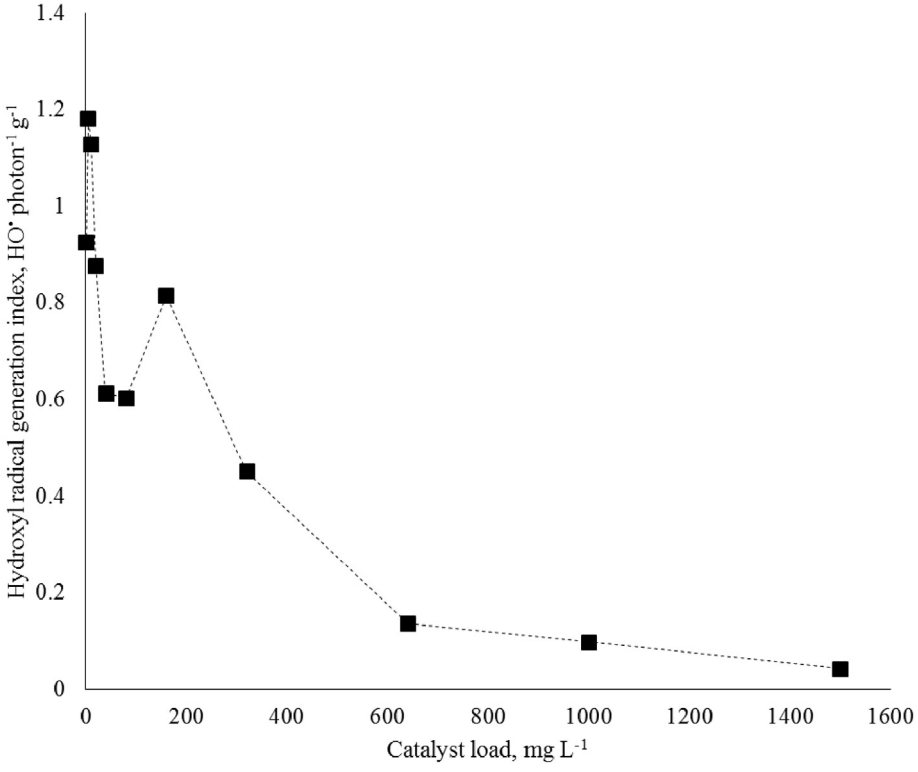

Fig. 11. Experimental values for OHI obtained using different loads of Aeroxide® P25.

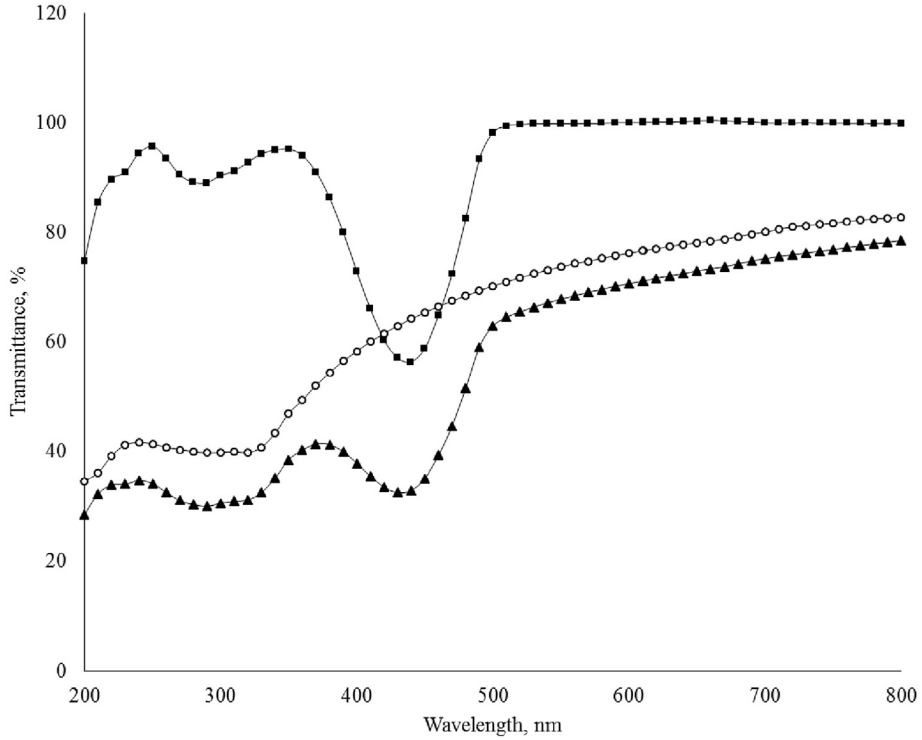

Fig. 12. Transmittance of solution with pNDA (10 μM, pH 6.20 ± 0.5 °C) —■—, TiO_2 (Aeroxide® P25, 20 mg L^{-1}) —○—, pNDA + TiO_2 (pNDA at 10 μM and TiO_2 at 20 mg L^{-1}) —▲—.

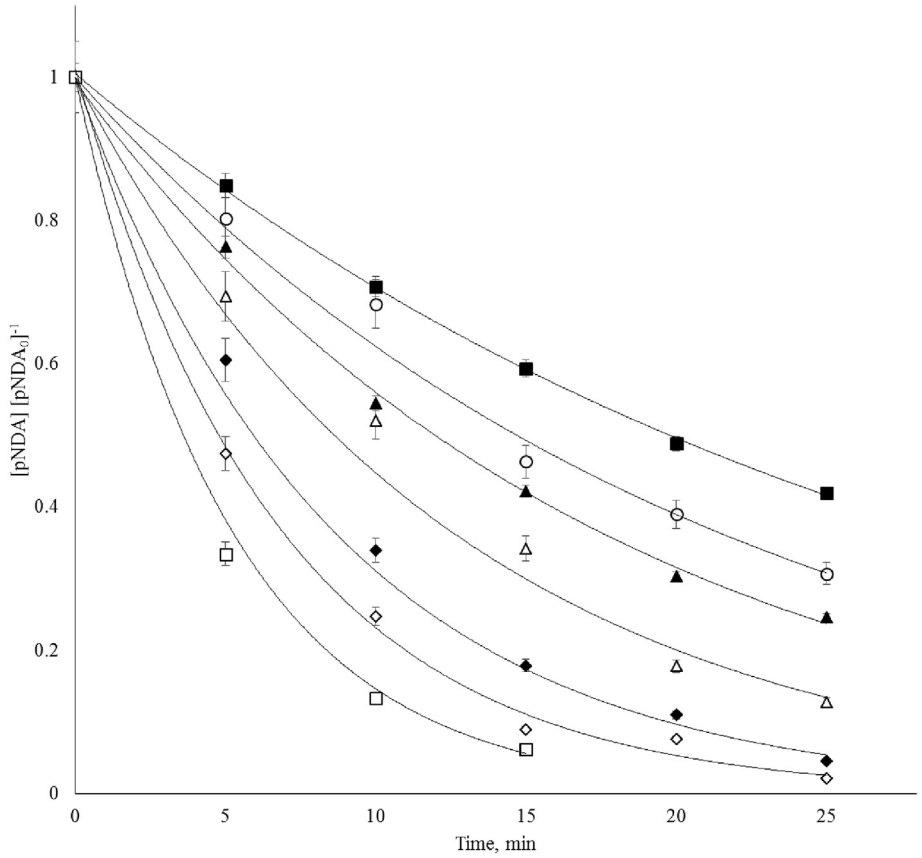

Fig. 13. Effect of temperature on photocatalytic pNDA bleaching (20 mg L^{-1}, Lamp GE F15T8 BLB) with pseudo-first-order model according Eq. (3).

Table 2
Temperature effects on photocatalytic kinetic reaction rate.

Temp, K	$pNDA_0$, μM	k_1, min^{-1}	Inverse fluence (cm^2 mJ^{-1})[a]	R^2	Half-life, min
278.15	7.65	0.04	(4.44×10^{-4})	0.999	17.3
283.15	7.62	0.05	(5.55×10^{-4})	0.989	13.9
288.15	7.37	0.06	(6.66×10^{-4})	0.997	11.6
293.15	7.65	0.08	(8.88×10^{-4})	0.985	8.7
303.15	7.62	0.11	(1.22×10^{-4})	0.972	6.3
313.15	8.18	0.15	(1.66×10^{-4})	0.977	4.6
323.15	7.83	0.19	(2.11×10^{-4})	0.994	3.6

[a] Inverse fluence was estimated using the incident fluence (not average fluence) rate computed from actinometry results.

Arrhenius-type equation and the Fermi level of electrons in a semiconductor. To demonstrate the effect of temperature on •OH radical production as input resource, pNDA photocatalytic bleaching was used in the photocatalytic system. The temperature range studied was from 5 to 50 °C and a photocatalyst load was 20 mg L^{-1}. The effect of temperature on •OH radical generation is shown in Fig. 13. The photocatalyst load of 20 mg L^{-1} was selected because the faster reaction (Table 1) minimized any changes in concentration due to solvent evaporation, which appeared negligible during the twenty-five minute reaction.

Generation of •OH radical increased with increasing temperature following the pseudo-first-order reaction as shown in Table 2.

The pseudo-first-order rate constant for •OH generation that was plotted and fitted using the Arrhenius model $k_1 = Ae^{-\frac{E_a}{R}\frac{1}{T}}$ in Fig. 14.

The Arrhenius plot of $ln\,(k_1)$ versus T^{-1} found a good correlation of experimental data with the equation $ln\,(k) = -3286.29\,T^{-1} + 8.58$ and $R^2 = 0.976$. Considering $R = 8.31446$ J $mol^{-1}K^{-1}$, the activation energy for the process was found to be −27323.77 J mol^{-1} and the frequency factor was 5312.56 min^{-1}. The Arrhenius equation obtained is shown in Equation (9).

$$k_1 = Ae^{-\frac{E_a}{R}\frac{1}{T}} = 5312.56e^{-3286.29\,\frac{1}{T}} \tag{9}$$

The increase in the pseudo-first-order rate constant with increasing temperature could be attributed to a more facile interfacial transfer of electrons and resulting reduction of the recombination rate of the photogenerated charge carriers, according to the e^- and h^+ system in Equation (10) (Liu et al., 2014):

$$e^{CB}_{TiO_2} + h^{VB}_{TiO_2} \leftrightarrow TiO_2, \quad v_{IT} = k_{IT}\left[e^{CB}_{TiO_2}\right]\left[h^{VB}_{TiO_2}\right] \tag{10}$$

where $e^{CB}_{TiO_2}$ is electron in conduction band, $h^{VB}_{TiO_2}$ is vacancies in valence band, v_{IT} is velocity of interfacial transfer, k_{IT} is the rate constant of the interfacial transfer. Knowing the photocatalytic ratio dependence on temperature could be operationally useful when an increased reaction rate is needed with an equal amount of photocatalyst or when using solar irradiance where not all photons

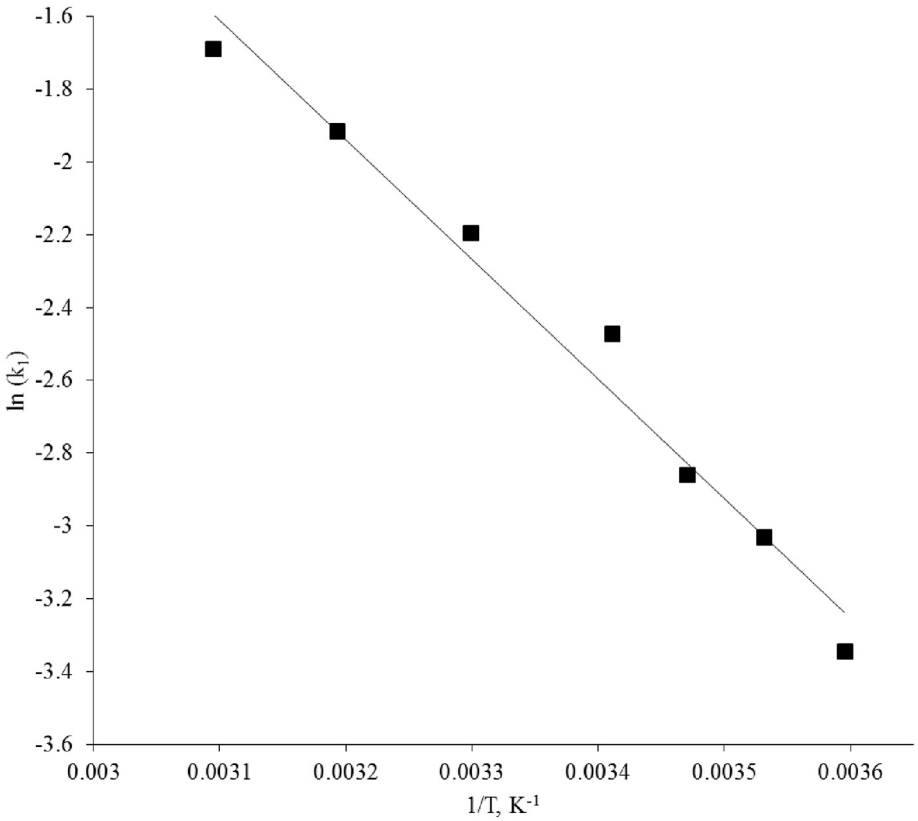

Fig. 14. Effect of temperature on the photocatalytic bleaching rate constant of pNDA (10 μM, pH 6) by TiO_2 Aeroxide® P25 (20 mg L^{-1}) under black light lamp (GE F15T8 BLB).

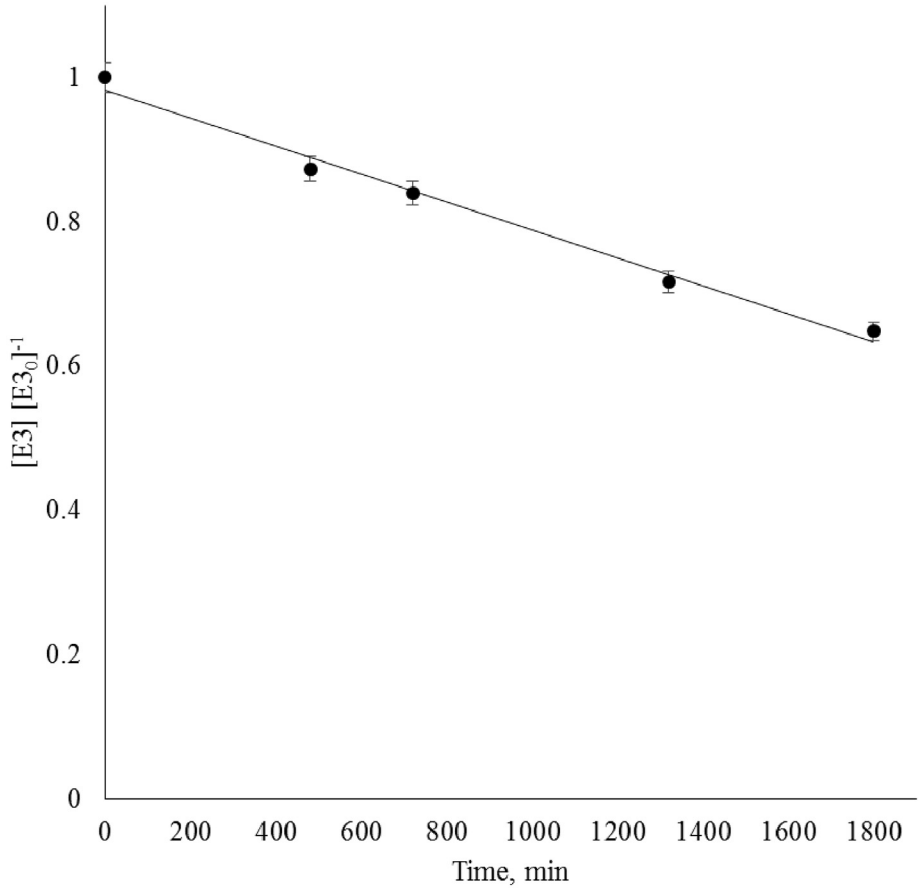

Fig. 15. E3 photolysis (10 μM, pH 6.20 ± 0.5 °C) under black light lamp (GE F15T8 BLB).

are able to be absorbed but temperature could be helpful to increase reaction kinetic rate.

3.4. Photolysis and photocatalytic degradation and mineralization of E3

To avoid misinterpreting E3 photocatalytic degradation and photolysis, a photolysis experiment was developed under lamp radiation without a catalyst. Estriol photolysis under a black light lamp (GE F15T8 BLB) was fit to a pseudo-first-order reaction modeled by the equation $\ln([E3]\ [E3_0]^{-1}) = -0.00024$ t, which obtained correlation coefficient of 0.997 as shown in Fig. 15.

Only 40% of E3 was degraded by photolysis after 30 h of irradiation. Other reports have found direct photolysis of E3 fitting with a pseudo-first-order kinetic value of 2.5×10^{-2} min^{-1} using a 20 W black light blue fluorescent lamp, and up to 9×10^{-2} min^{-1} using germicidal radiation lamps (Coleman et al., 2007). It is well-known that only light absorbed by the system can cause a chemical change (Grotthus-Draper law). Germicidal lamps have emission peaks at 254 nm, the point at which E3 has significant molar absorption (as shown in Fig. 2a), whereas black light emission lamps, which were used in this study, have emission peaks at 387 nm (Fig. 4), the point at which E3 molar absorption is almost null.

While several different ROS may be produced during TiO_2 UV irradiation, hydroxyl radicals have been reported as the most significant ROS being produced and capable to perform organic pollutants oxidation. pNDA experiments were useful for obtaining the best conditions for resource efficiency in •OH radical generation in the studied photocatalytic system, the best conditions for the system were used to evaluate E3 degradation and mineralization. Degradation refers to changes in E3 moiety that can produce a reduction in detection for HPLC analysis, whereas mineralization refers to the conversion of E3 into CO_2 as followed by TOC analysis. The experimental conditions chosen for E3 photocatalytic degradation and mineralization were a catalyst load in the range of 20–160 mg L^{-1}, a temperature of 20 °C, and a photon flux of 28.1 μEinstein min^{-1}. To trade-off with photocatalytic resources, the TiO_2 photocatalyst loads were in the range of 20–160 mg L^{-1}, conditions under which the catalyst dosage was sufficient for ready degradation of E3 but below catalyst saturation. The effect of catalyst loading for E3 degradation is plotted in Fig. 16a, and mineralization is shown in Fig. 16b.

When the E3 solution was degraded using TiO_2 and UV radiation (Fig. 16a), the initial absorption of the solution was observed to decrease as a function of time following pseudo-first-order kinetics (see Table 3). Control experiments performed using a hydroxyl radical scavenger (methanol) at different concentrations (data not shown) were performed to evaluate the potential effect of other ROS, different from HO•, in the photocatalytic degradation. It was observed that the addition of the hydroxyl radical scavenger significantly depleted the photocatalytic reaction process, suggesting these species as the main involved in E3 photocatalytic degradation. The change in molar absorption detected by HPLC was probably because of E3 modification by exposure to the •OH radical produced as proposed by Ohko et al. (2002) and Coleman et al. (2004, 2005a, 2005b) that found that estrogen degradation occurs via abstraction of the benzylic hydrogen by the •OH radical or via the attack of the •OH group to form quinone-type compounds.

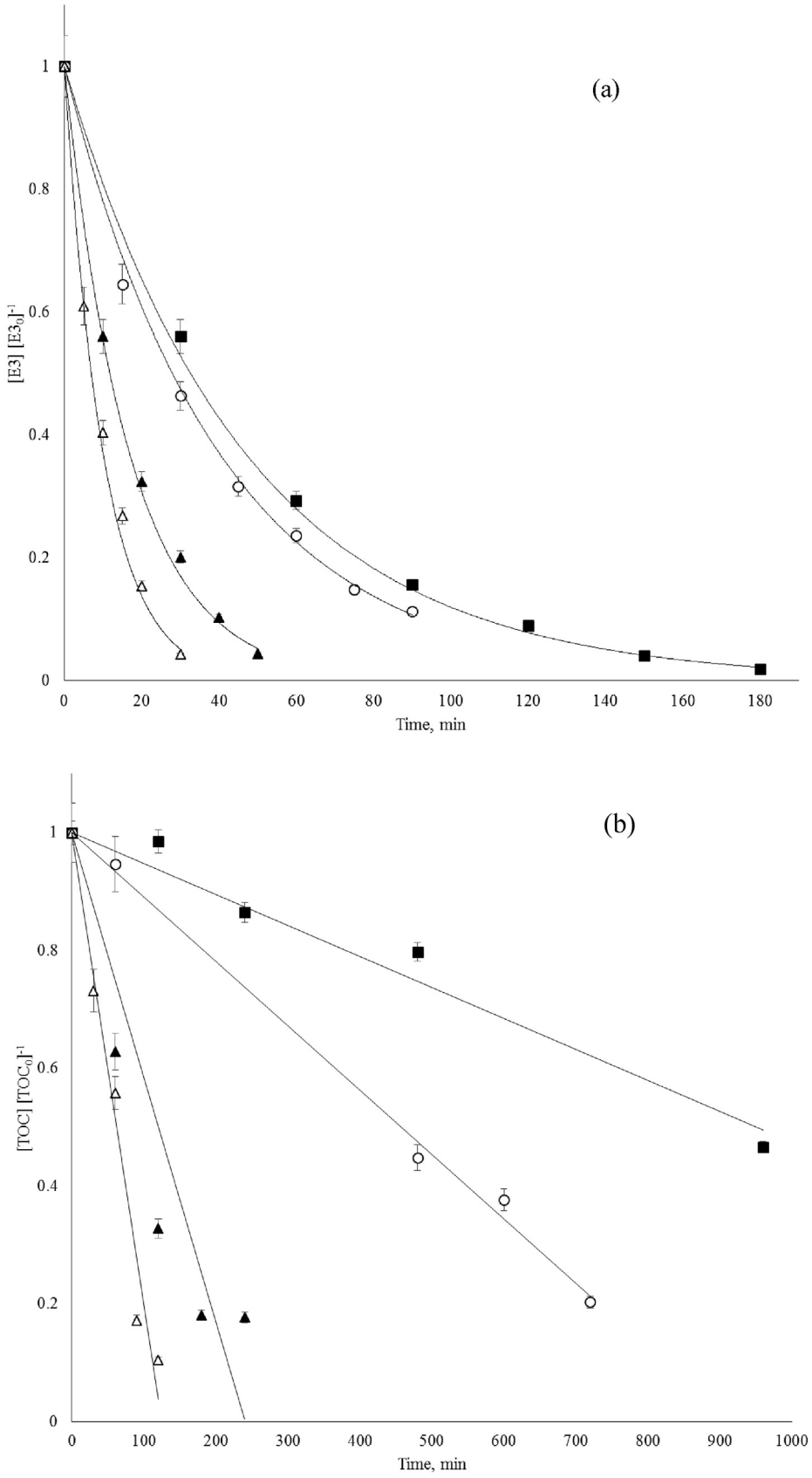

Fig. 16. Catalyst load effect on a) degradation with pseudo-first order model (-) and b) mineralization with zero-order model (- - -) of E3 (10 μM, pH 6.20 ± 0.5 °C) under black light lamp (GE F15T8 BLB). Experimental data: ■ 20 mg L^{-1}, ○ 40 mg L^{-1}, ▲ 80 mg L^{-1}, and △ 160 mg L^{-1}.

Table 3
Kinetic reaction rate for mineralization and degradation of estriol (E3) using Aeroxide® TiO_2.

Catalyst load mg L^{-1}	Mineralization			Degradation					
	k_1, min^{-1}	Inverse fluence cm^2 mJ^{-1} [a]	R^2	k_1, min^{-1}	Inverse fluence cm^2 mJ^{-1} [a]	R^2	Initial velocity rate, μM_{E3} min^{-1}	Half time, min	Initial degradation efficiency (IDE)
20	0.0005	5.55×10^{-6}	0.969	0.021	2.33×10^{-4}	0.996	0.21	33.01	2.4
40	0.0011	1.22×10^{-5}	0.996	0.0248	2.66×10^{-4}	0.996	0.23	27.9	3.5
80	0.0042	4.66×10^{-5}	0.837	0.0589	6.54×10^{-4}	0.989	0.56	11.8	2.7
160	0.0080	8.88×10^{-5}	0.9683	0.0989	1.09×10^{-3}	0.987	0.91	7.01	4.0

Note: Lamp type: F15T8BLB GE W; $\lambda_{max} = 365$ nm; radiative flow = 28.1 μEinstein min^{-1}; radiative intensity = 1500 μWcm^{-2}; temperature = 20.0 ± 0.04 °C; and pH = 6.
[a] Inverse fluence was estimated using the incident fluence (not average fluence) rate computed from actinometry results.

Total organic carbon was measured (Fig. 16b) and it was observed that E3 mineralization was considerably slower than E3 degradation (Fig. 16a).

The E3 mineralization rate was also fitted to a pseudo-first-order model. The difference between degradation and mineralization rates was likely because of hydroxyl insertion, reduction, or opening of the ring at the estrogen moiety changing the HPLC detection without significantly changing the TOC measurement. The E3 mineralization rate follows a slow degradation rate, probably because of the slow breakdown of further intermediate products of the initial photocatalytic degradation, which has also been suggested for other similar estrogenic molecules e.g., ethynylestradiol (EE2) by Li and Sun (2014) and estradiol (E2) by Mai et al. (2008).

To evaluate the resource efficiency for E3 degradation, initial degradation efficiency (IDE) was proposed as a measurement that describes the relationship between the amount of •OH radical produced and the amount of E3 degradation at the initial condition which is in agreement with Equation (11).

$$IDE = \frac{\left.\frac{d(\cdot OH)}{dt}\right|_{t=0}}{\left.\frac{d(E3)}{dt}\right|_{t=0}} = \frac{r_{0,\cdot OH}}{r_{0,E3}} \tag{11}$$

where $r_{0,\cdot OH}$ is initial velocity rate of OH generation and $r_{0,E3}$ initial velocity rate of E3 degradation. The IDE represents the amount of •OH radicals that should be produced in the system to degrade one E3 molecule at an initial time (t = 0). The IDE should be obtained at initial degradation time, when all molecules in the systems are E3 molecules, because after initial time, there may be E3 and additional degradation by-products because of unselective attack by the •OH radicals.

The initial •OH generation in Table 1 and the initial degradation rate of E3 in Table 3 were used to obtain the IDE values that are also shown in Table 3. The higher IDE values mean that more •OH radical were produced in the system to degrade one E3 molecule. The lowest IDE value found was approximately 2.4 which means that this amount of •OH radicals needs to be produced in the photocatalytic system before detecting any modification in the E3 chemicals structure. Differences in IDE values were related to the efficient transport of E3 molecules to the catalyst surface or the effect of the catalyst surface charge.

4. Conclusions

This research assessed the relationship between the amount of •OH radical generation and estriol degradation and proposed two indices to evaluate the efficient use of resources. As efficiency values, OHI is more effective as the value increases, whereas IDE is better as the value decreases. This relationship can be useful for comparing operational conditions to understand the trade-offs and supply recourse in photocatalytic operations and upscaling the photocatalytic process from lab scale to pilot scale. Our main findings are the following:

(1) It was demonstrated that E3 can be degraded and mineralized under convenient experimental conditions previously determined using the •OH probe pNDA.
(2) It was confirmed that pNDA can be useful as a scavenger to determine •OH generation.
(2) Increasing hydroxyl radical generation by increasing temperature is fairly well fitted using the Arrhenius model.
(4) The OHI and temperature function values could be beneficial for photoreactor upscaling and trade-offs with materials, energy, and degradation rate.
(5) The IDE could be associated with transport phenomena, superficial catalyst charge, molecule charge, and adsorption phenomena.
(6) The OHI and IDE could be used to evaluate the performance of a photocatalyst and set up a photoreactor in lab-scale and upscaling experiments.

Knowing the dependence of temperature and the pseudo-first-order constant of •OH radical generation allows us to consider an additional resource efficiency value for the trade-offs between the energy supply, photon flux, catalyst loading, and degradation rate. We suggest that the goals of future studies should include: 1) modeling uncontrolled temperature experiments to confirm the accuracy of using the Arrhenius model to predict •OH generation using TiO_2, 2) determining the •OH generation index and initial degradation efficiency of E3 in a continuous photocatalytic reactor using lamps that are set up axially, and 3) demonstrating that photolysis and photocatalytic processes should both be considered to significantly contribute to the overall organic degradation when the catalyst load is low and the molecule studied has a high absorption at the main emission wavelength of the irradiation source.

Acknowledgments

The Aeroxide® P25 Evonik catalyst used for this work was provided by Intertrade S.A. de C.V., the supplier of Evonik Industries in Mexico. This material is based upon work supported in part by the National Science Foundation (grant IIA-1301726) and by the US-EPA P3 program (Grant no. 83676801). The authors thank Dr. M.A. Quiroz Alfaro for his excellent technical help and allowing the use of materials and equipment at the UDLAP's electrochemical lab. The authors are also grateful to Ms. Nicole Damon (DRI) for her editorial review.

References

Barashkov, N.N., Eisenberg, D., Eisenberg, S., Shegebaeva, G.S., Irgibaeva, I.S., Barashkova, I.I., 2010. Electrochemical chlorine-free AC disinfection of water contaminated with Salmonella typhimurium bacteria. Russ. J. Electrochem 46, 306–311. http://dx.doi.org/10.1134/S1023193510030079.

Benotti, M.J., Stanford, B.D., Wert, E.C., Snyder, S.A., 2009. Evaluation of a photocatalytic reactor membrane pilot system for the removal of pharmaceuticals and endocrine disrupting compounds from water. Water Res. 43, 1513–1522. http://dx.doi.org/10.1016/j.watres.2008.12.049.

Bors, W., Michel, C., Saran, M., 1979. On the nature of biochemically generated hydroxyl radicals. Studies using the bleaching of p-nitrosodimethylaniline as a direct assay method. Eur. J. Biochem. 95, 621–627. http://dx.doi.org/10.1111/j.1432-1033.1979.tb13003.x.

Brezonik, P., Arnold, W., 2011. Water Chemistry: an Introduction to the Chemistry of Natural and Engineered Aquatic Systems, first ed. Oxford University Press, New York, NY.

Brezová, V., Tarábek, P., Dvoranová, D., Staško, A., Biskupič, S., 2003. EPR study of photoinduced reduction of nitroso compounds in titanium dioxide suspensions. J. Photochem. Photobiol. A Chem. 155, 179–198. http://dx.doi.org/10.1016/S1010-6030(02)00357-X.

Cavalieri, E., Frenkel, K., Liehr, J.G., Rogan, E., Roy, D., 2000. Estrogens as endogenous genotoxic agents-DNA adducts and mutations. J. Natl. Cancer Inst. Monogr. 75–93. http://dx.doi.org/10.1093/oxfordjournals.jncimonographs.a024247.

Chen, C.-Y., Wen, T.-Y., Wang, G.-S., Cheng, H.-W., Lin, Y.-H., Lien, G.-W., 2007. Determining estrogenic steroids in Taipei waters and removal in drinking water treatment using high-flow solid-phase extraction and liquid chromatography/tandem mass spectrometry. Sci. Total Environ. 378, 352–365. http://dx.doi.org/10.1016/j.scitotenv.2007.02.038.

Coleman, H.M., Abdullah, M.I., Eggins, B.R., Palmer, F.L., 2005a. Photocatalytic degradation of 17[beta]-oestradiol, oestriol and 17[alfa]-ethynyloestradiol in water monitored using fluorescence spectroscopy. Appl. Catal. B Environ. 55, 23–30. http://dx.doi.org/10.1016/j.apcatb.2004.07.004.

Coleman, H.M., Chiang, K., Amal, R., 2005b. Effects of Ag and Pt on photocatalytic degradation of endocrine disrupting chemicals in water. Chem. Eng. J. 113, 65–72. http://dx.doi.org/10.1016/j.cej.2005.07.014.

Coleman, H.M., Routledge, E.J., Sumpter, J.P., Eggins, B.R., Byrne, J.A., 2004. Rapid loss of estrogenicity of steroid estrogens by UVA photolysis and photocatalysis over an immobilised titanium dioxide catalyst. Water Res. 38, 3233–3240. http://dx.doi.org/10.1016/j.watres.2004.04.021.

Coleman, H.M., Vimonses, V., Leslie, G., Amal, R., 2007. Removal of contaminants of concern in water using advance oxidation techniques. Water Sci. Technol. 55, 301–306. http://dx.doi.org/10.2166/wst.2007.421.

Coleman, Eggins, B., Byrne, J.A., Palmer, F.L., King, E., 2000. Photocatalytic degradation of 17-β-oestradiol on immobilised TiO_2. Appl. Catal. B Environ. 24, L1–L5. http://dx.doi.org/10.1016/S0926-3373(99)00091-0.

Czech, B., Rubinowska, K., 2013. TiO_2-assisted photocatalytic degradation of diclofenac, metoprolol, estrone and chloramphenicol as endocrine disruptors in water. Adsorption 19, 619–630. http://dx.doi.org/10.1007/s10450-013-9485-8.

Desbrow, C., Routledge, E.J., Brighty, G.C., Sumpter, J.P., Waldock, M., 1998. Identification of estrogenic chemicals in STW effluent. 1. Chemical fractionation and in vitro biological screening. Environ. Sci. Technol. 32, 1549–1558. http://dx.doi.org/10.1021/es9707973.

Dimitroula, H., Daskalaki, V.M., Frontistis, Z., Kondarides, D.I., Panagiotopoulou, P., Xekoukoulotakis, N.P., Mantzavinos, D., 2012. Solar photocatalysis for the abatement of emerging micro-contaminants in wastewater: synthesis, characterization and testing of various TiO_2 samples. Appl. Catal. B Environ. 117–118, 283–291. http://dx.doi.org/10.1016/j.apcatb.2012.01.024.

Dimogerontas, G., Liapi, C., 2014. Endocrine disruptors (Xenoestrogens): an overview. In: Eliades, T., Eliades, G. (Eds.), Plastics in Dentistry and Estrogenicity: a Guide to Safe Practice. Springer Berlin Heidelberg, Berlin, Heidelberg, pp. 3–48. http://dx.doi.org/10.1007/978-3-642-29687-1_1.

Fanourgiakis, S., Frontistis, Z., Chatzisymeon, E., Venieri, D., Mantzavinos, D., 2014. Simultaneous removal of estrogens and pathogens from secondary treated wastewater by solar photocatalytic treatment. Glob. Nest J. 16, 543–552.

Farhataziz, A.B.R., 1977. Selected Specific Rates of Reactions of Transients from Water in Aqueous Solutions III: Hydroxyl Radical and Perhydroxyl Radical and Their Radical Ions. Washington.

Feng, C., Sugiura, N., Shimada, S., Maekawa, T., 2003. Development of a high performance electrochemical wastewater treatment system. J. Hazard. Mater 103, 65–78. http://dx.doi.org/10.1016/S0304-3894(03)00222-X.

Fernández-Ibáñez, P., De Las Nieves, F.J., Malato, S., 2000. Titanium dioxide/electrolyte solution interface: electron transfer phenomena. J. Colloid Interface Sci. 227, 510–516 doi:10.1006.

Fischer, A.M., Kliger, D.S., Winterle, J.S., Mill, T., 1985. Direct observation of phototransients in natural waters. Chemosphere 14, 1299–1306. http://dx.doi.org/10.1016/0045-6535(85)90150-X.

Frontistis, Z., Drosou, C., Tyrovola, K., Mantzavinos, D., Fatta-Kassinos, D., Venieri, D., Xekoukoulotakis, N.P., 2012. Experimental and modeling studies of the degradation of estrogen hormones in aqueous TiO_2 suspensions under simulated solar radiation. Ind. Eng. Chem. Res. 51, 16552–16563. http://dx.doi.org/10.1021/ie300561b.

Fujishima, A., Zhang, X., Tryk, D.A., 2007. Heterogeneous photocatalysis: from water photolysis to applications in environmental cleanup. Int. J. Hydrogen Energy 32, 2664–2672. http://dx.doi.org/10.1016/j.ijhydene.2006.09.009.

Giraldo, A.L., Peñuela, G.A., Torres-Palma, R.A., Pino, N.J., Palominos, R.A., Mansilla, H.D., 2010. Degradation of the antibiotic oxolinic acid by photocatalysis with TiO_2 in suspension. Water Res. 44, 5158–5167. http://dx.doi.org/10.1016/j.watres.2010.05.011.

Guitaya, L., Drogui, P., Blais, J.F., 2014. In situ reactive oxygen species production for tertiary wastewater treatment. Environ. Sci. Pollut. Res. Int. 22, 7025–7036. http://dx.doi.org/10.1007/s11356-014-3907-3.

Han, J., Liu, Y., Singhal, N., Wang, L., Gao, W., 2012. Comparative photocatalytic degradation of estrone in water by ZnO and TiO_2 under artificial UVA and solar irradiation. Chem. Eng. J. 213, 150–162. http://dx.doi.org/10.1016/j.cej.2012.09.066.

Hapeshi, E., Achilleos, A., Vasquez, M.I., Michael, C., Xekoukoulotakis, N.P., Mantzavinos, D., Kassinos, D., 2010. Drugs degrading photocatalytically: kinetics and mechanisms of ofloxacin and atenolol removal on titania suspensions. Water Res. 44, 1737–1746. http://dx.doi.org/10.1016/j.watres.2009.11.044.

Hileman, B., 1994. Environmental estrogens linked to reproductive abnormalities. Cancer. Chem. Eng. News Arch. 72, 19–23. http://dx.doi.org/10.1021/cen-v072n005.p019.

Hurwitz, A.R., Liu, S.T., 1977. Determination of aqueous solubility and pKa values of estrogens. J. Pharm. Sci. 66, 624–627 doi:soly estrogen acidity estrogen estrogen soly acidity.

Karpova, T., Preis, S., Kallas, J., 2007. Selective photocatalytic oxidation of steroid estrogens in water treatment: urea as co-pollutant. J. Hazard. Mater 146, 465–471. http://dx.doi.org/10.1016/j.jhazmat.2007.04.047.

Kim, C., Park, H.J., Cha, S., Yoon, J., 2013. Facile detection of photogenerated reactive oxygen species in TiO_2 nanoparticles suspension using colorimetric probe-assisted spectrometric method. Chemosphere 93, 2011–2015. http://dx.doi.org/10.1016/j.chemosphere.2013.07.023.

Komagoe, K., Takeuchi, H., Katsu, T., 2008. Oxygen electrode as a new tool to evaluate hydroxyl radical-scavenging ability. Sens. Actuators, B Chem. 134, 516–520. http://dx.doi.org/10.1016/j.snb.2008.05.033.

Kostich, M., Flick, R., Martinson, J., 2013. Comparing predicted estrogen concentrations with measurements in US waters. Environ. Pollut. 178, 271–277. http://dx.doi.org/10.1016/j.envpol.2013.03.024.

Kraljic, I., Trumbore, C.N., 1965. p-Nitrosodimethylaniline as an OH radical scavenger in radiation chemistry. J. Am. Chem. Soc. 87, 2547–2550. http://dx.doi.org/10.1021/ja01090a004.

Kuch, H.M., Ballschmiter, K., 2001. Determination of endocrine-disrupting phenolic compounds and estrogens in surface and drinking water by HRGC-(NCI)-MS in the picogram per liter range. Environ. Sci. Technol. 35, 3201–3206. http://dx.doi.org/10.1021/es010034m.

Kuhn, H.J., Braslavsky, S.E., Schmidt, R., 2004. Chemical actinometry (IUPAC technical report). Pure Appl. Chem. 76, 2105–2146. http://dx.doi.org/10.1351/pac200476122105.

Kushwaha, H.S., Parmesh, G., Vaish, R., Varma, K.B.R., 2015. TiO_2 microcrystallized glass plate mediated photocatalytic degradation of estrogenic pollutant in water. J. Non. Cryst. Solids 408, 13–17. http://dx.doi.org/10.1016/j.jnoncrysol.2014.10.007.

Kwon, B.G., Ryu, S., Yoon, J., 2009. Determination of hydroxyl radical rate constants in a continuous flow system using competition kinetics. J. Ind. Eng. Chem. 15, 809–812. http://dx.doi.org/10.1016/j.jiec.2009.09.004.

Li, S., Sun, W., 2014. Photocatalytic degradation of 17α-ethinylestradiol in mono- and binary systems of fulvic acid and Fe(III): application of fluorescence excitation/emission matrixes. Chem. Eng. J. 237, 101–108. http://dx.doi.org/10.1016/j.cej.2013.10.002.

Li Puma, G., Puddu, V., Tsang, H.K., Gora, A., Toepfer, B., 2010. Photocatalytic oxidation of multicomponent mixtures of estrogens (estrone (E1), 17β-estradiol (E2), 17α-ethynylestradiol (EE2) and estriol (E3)) under UVA and UVC radiation: photon absorption, quantum yields and rate constants independent of photon absorp. Appl. Catal. B Environ. 99, 388–397. http://dx.doi.org/10.1016/j.apcatb.2010.05.015.

Liu, B., Zhao, X., Terashima, C., Fujishima, A., Nakata, K., 2014. Thermodynamic and kinetic analysis of heterogeneous photocatalysis for semiconductor systems. Phys. Chem. Chem. Phys. 16, 8751–8760. http://dx.doi.org/10.1039/c3cp55317e.

Liu, Z., Lu, G., Yin, H., Dang, Z., 2015. Do we underestimate the concentration of estriol in raw municipal wastewater? Environ. Sci. Pollut. Res. 22, 4753–4758. http://dx.doi.org/10.1007/s11356-014-3981-6.

Lorenz, R.D., 2014. A simple webcam spectrograph. Am. J. Phys. 82, 169–173. http://dx.doi.org/10.1119/1.4853835.

Mai, J., Sun, W., Xiong, L., Liu, Y., Ni, J., 2008. Titanium dioxide mediated photocatalytic degradation of 17beta-estradiol in aqueous solution. Chemosphere 73, 600–606. http://dx.doi.org/10.1016/j.chemosphere.2008.05.073.

Maki, T., Soh, N., Fukaminato, T., Nakajima, H., Nakano, K., Imato, T., 2009. Perylenebisimide-linked nitroxide for the detection of hydroxyl radicals. Anal. Chim. Acta 639, 78–82. http://dx.doi.org/10.1016/j.aca.2009.02.044.

Malygina, T., Preis, S., Kallas, J., 2005. The role of pH in aqueous photocatalytic oxidation of beta-estradiol. Int. J. Photoenergy 7, 187–191.

Mao, K., Li, Y., Zhang, H., Zhang, W., Yan, W., 2013. Photocatalytic degradation of 17α-ethinylestradiol and inactivation of Escherichia coli using Ag-Modified TiO_2 nanotube arrays. Clean. – Soil, Air, Water 41, 455–462. http://dx.doi.org/10.1002/clen.201100698.

Martínez-Huitle, C.A., Quiroz, M.A., Comninellis, C., Ferro, S., De Battisti, A., 2004. Electrochemical incineration of chloranilic acid using Ti/IrO_2, Pb/PbO_2 and Si/BDD electrodes. Electrochim. Acta 50, 949–956. http://dx.doi.org/10.1016/j.electacta.2004.07.035.

Matozzo, V., Gagné, F., Marin, M.G., Ricciardi, F., Blaise, C., 2008. Vitellogenin as a biomarker of exposure to estrogenic compounds in aquatic invertebrates: a review. Environ. Int. http://dx.doi.org/10.1016/j.envint.2007.09.008.

Mboula, V.M., Héquet, V., Andrés, Y., Gru, Y., Colin, R., Doña-Rodríguez, J.M., Pastrana-Martínez, L.M., Silva, A.M.T., Leleu, M., Tindall, A.J., Mateos, S., Falaras, P., 2015. Photocatalytic degradation of estradiol under simulated solar light and

assessment of estrogenic activity. Appl. Catal. B Environ. 162, 437–444. http://dx.doi.org/10.1016/j.apcatb.2014.05.026.
Mizuguchi, T., Sadaka, S., Ogasawara, C., Shimada, K., 2006. Determination of the effect of hydrogen peroxide on photocatalytic degradation of estrogen using HPLC. J. Liq. Chromatogr. Relat. Technol. 29, 903–911. http://dx.doi.org/10.1080/10826070500531458.
Montalti, M., Credi, A., Prodi, L., Gandolfi, T., 2006. Handbook of Photochemistry, 3rd ed. CRC Press, New York, NY.
Muff, J., Bennedsen, L.R., Søgaard, E.G., 2011. Study of electrochemical bleaching of p-nitrosodimethylaniline and its role as hydroxyl radical probe compound. J. Appl. Electrochem 41, 599–607. http://dx.doi.org/10.1007/s10800-011-0268-1.
Murov, S.L., Carmichael, I., Hug, G.L., 1993. Handbook of Photochemistry, second ed. CRC Press, New York, NY.
Nadal, A., Alonso-Magdalena, P., Soriano, S., Quesada, I., Ropero, A.B., 2009. The pancreatic Beta-cell as a target of estrogens and xenoestrogens: implications for blood glucose homeostasis and diabetes. Mol. Cell. Endocrinol. http://dx.doi.org/10.1016/j.mce.2009.02.016.
Nakashima, T., Ohko, Y., Kubota, Y., Fujishima, A., 2003. Photocatalytic decomposition of estrogens in aquatic environment by reciprocating immersion of TiO_2-modified polytetrafluoroethylene mesh sheets. J. Photochem. Photobiol. A Chem. 160, 115–120. http://dx.doi.org/10.1016/S1010-6030(03)00229-6.
Nakashima, T., Ohko, Y., Tryk, D.A., Fujishima, A., 2002. Decomposition of endocrine-disrupting chemicals in water by use of TiO2 photocatalysts immobilized on polytetrafluoroethylene mesh sheets. J. Photochem. Photobiol. A Chem. 151, 207–212. http://dx.doi.org/10.1016/S1010-6030(02)00139-9.
Nakata, K., Ochiai, T., Murakami, T., Fujishima, A., 2012. Photoenergy conversion with TiO_2 photocatalysis: new materials and recent applications. Electrochim. Acta 84, 103–111. http://dx.doi.org/10.1016/j.electacta.2012.03.035.
Nasuhoglu, D., Berk, D., Yargeau, V., 2012. Photocatalytic removal of 17α-ethinylestradiol (EE2) and levonorgestrel (LNG) from contraceptive pill manufacturing plant wastewater under UVC radiation. Chem. Eng. J. 185–186, 52–60. http://dx.doi.org/10.1016/j.cej.2012.01.012.
Nosaka, Y., Nosaka, A.Y., 2013. Identification and roles of the active species generated on various photocatalysts. In: Photocatalysis and Water Purification: from Fundamentals to Recent Applications, pp. 3–24. http://dx.doi.org/10.1002/9783527645404.ch1.
Oetken, M., Bachmann, J., Schulte-Oehlmann, U., Oehlmann, J., 2004. Evidence for endocrine disruption in invertebrates. Int. Rev. Cytol. http://dx.doi.org/10.1016/S0074-7696(04) 36001–8.
Ohko, Y., Iuchi, K., Niwa, C., Tatsuma, T., Nakashima, T., Iguchi, T., Kubota, Y., Fujishima, A., 2002. 17β-Estradiol degradation by TiO_2 photocatalysis as a means of reducing estrogenic activity. Environ. Sci. Technol. 36, 4175–4181. http://dx.doi.org/10.1021/es011500a.
Parker, C., 1953. A new sensitive chemical actinometer. I. Some trials with potassium ferrioxalate. Proc. R. Soc. Lond. A. Math. Phys. Sci. 220, 104–116. http://dx.doi.org/10.1098/rspa.1953.0175.
Pastore, D., Trono, D., Padalino, L., Di Fonzo, N., Passarella, S., 2000. p-Nitrosodimethylaniline (RNO) bleaching by soybean lipoxygenase-1. Biochemical characterization and coupling with oxodiene formation. Plant Physiol. Biochem. 38, 845–852. http://dx.doi.org/10.1016/S0981-9428(00)01194-3.
Quiroz, M.A., Sanchez-Salas, J.L., Reyna, S., Bandala, E.R., Peralta-Hernandez, J.M., Martinez-Huitle, C.A., 2014. Degradation of 1-hydroxy-2,4-dinitrobenzene from aqueous solutions by electrochemical oxidation: role of anodic material. J. Hazard. Mater 268, 6–13. http://dx.doi.org/10.1016/j.jhazmat.2013.12.050.
Ramirez-Sanchez, I.M., Mendez-Rojas, M.A., Bandala, E.R., 2017. CHAPTER 25 photocatalytic degradation of natural and synthetic estrogens with semiconducting nanoparticles. In: Advanced Environmental Analysis: Applications of Nanomaterials{,}, vol. 2. The Royal Society of Chemistry, pp. 153–177. http://dx.doi.org/10.1039/9781782629139-00153.
Serpone, N., 1997. Relative photonic efficiencies and quantum yields in heterogeneous photocatalysis. J. Photochem. Photobiol. A Chem. 104, 1–12. http://dx.doi.org/10.1016/S1010-6030(96)04538-8.
Silva, C.P., Otero, M., Esteves, V., 2012. Processes for the elimination of estrogenic steroid hormones from water: a review. Environ. Pollut. 38–58. http://dx.doi.org/10.1016/j.envpol.2012.02.002.
Simonsen, M.E., Muff, J., Bennedsen, L.R., Kowalski, K.P., Søgaard, E.G., 2010. Photocatalytic bleaching of p-nitrosodimethylaniline and a comparison to the performance of other AOP technologies. J. Photochem. Photobiol. A Chem. 216, 244–249. http://dx.doi.org/10.1016/j.jphotochem.2010.07.008.
Souza, M.S., Hallgren, P., Balseiro, E., Hansson, L.A., 2013. Low concentrations, potential ecological consequences: synthetic estrogens alter life-history and demographic structures of aquatic invertebrates. Environ. Pollut. 178, 237–243. http://dx.doi.org/10.1016/j.envpol.2013.03.038.
Sun, M., Ru, X.R., Zhai, L.F., 2015. In-situ fabrication of supported iron oxides from synthetic acid mine drainage: high catalytic activities and good stabilities towards electro-Fenton reaction. Appl. Catal. B Environ. 165, 103–110. http://dx.doi.org/10.1016/j.apcatb.2014.09.077.
Tanizaki, T., Kadokami, K., Shinohara, R., 2002. Catalytic photodegradation of endocrine disrupting chemicals using titanium dioxide photosemiconductor thin films. Bull. Environ. Contam. Toxicol. 68, 732–739. http://dx.doi.org/10.1007/s001280315.
Widiatmoko, E., Widayani, Budiman, M., Abdullah, M., Khairurrijal, 2011. A simple spectrophotometer using common materials and a digital camera. Phys. Educ. 46, 332–339. http://dx.doi.org/10.1088/0031-9120/46/3/014.
Williams, E.S., Brooks, B.W., 2012. Human pharmaceuticals in the environment: current and future perspectives. In: Brooks, W.B., Huggett, B.D. (Eds.). Springer New York, New York, NY, pp. 167–224. http://dx.doi.org/10.1007/978-1-4614-3473-3_8.
Ying, G.G., Kookana, R.S., Ru, Y.J., 2002. Occurrence and fate of hormone steroids in the environment. Environ. Int. http://dx.doi.org/10.1016/S0160-4120(02)00075-2.
Zang, L., Qu, P., Zhao, J., Shen, T., Hidaka, H., 1997. Photocatalytic bleaching of p-nitrosodimethylaniline in TiO_2 aqueous suspensions: a kinetic treatment involving some primary events photoinduced on the particle surface. J. Mol. Catal. A Chem. 120, 235–245. http://dx.doi.org/10.1016/S1381-1169(96)00404-9.
Zhang, W.L., Li, Y., Wu, Q.Y., Hu, H.Y., 2012. Removal of endocrine-disrupting compounds, estrogenic activity, and Escherichia coliform from secondary effluents in a TiO_2-coated photocatalytic reactor. Environ. Eng. Sci. 29, 195–201. http://dx.doi.org/10.1089/ees.2010.0387.